Efficiency of CryoFILL liquefaction tests

A Kashani[1*], R Grotenrath[2], K Yamashita[3], D Hauser[2], R Balasubramaniam[4] and W Johnson[2]

[1]ASRC Federal, Moffett Field, CA, 94035, USA
[2]NASA Glenn Research Center, Cleveland, OH, 44135, USA
[3] HX5, Cleveland, OH, 44135, USA
[4]Case Western Reserve University, Cleveland, OH, 44135, USA

[*]E-mail: ali.kashani@nasa.gov

Abstract. To demonstrate a technique for liquefaction of gaseous oxygen that will be produced on the Lunar or Martian surface the Cryogenic Fluid In-situ Liquefaction for Landers (CryoFILL) tests were conducted at NASA. The test setup included a 2.1 cubic meter tank with a broad area cooling (BAC) network. A commercial cryocooler provided cooling to the BAC working fluid. Steady state and transient liquefaction tests were conducted during the test series. A thermal model of the CryoFILL tank and its BAC system was developed in Thermal Desktop to simulate the experimental runs. An efficiency is calculated for all the liquefaction tests performed under the CryoFILL test series. This efficiency is a measure of the liquefaction process in the broad area cooling tank, and not an overall system efficiency that would include the cryocooler/heat exchanger system.

1. Introduction

NASA has been developing technologies for the production and storage of propellants on the surface of Mars and the Moon. The method considered for liquefaction of gases produced through in-situ resource utilization is Broad Area Cooling (BAC). In broad area cooling, gaseous helium or neon is circulated through tubes attached with good thermal contact to the outside surface of the propellant tank [1]. The BAC gas is cooled by a cryocooler prior to removing heat from the tank and thereby liquefying the gas flowing into the tank.

The Cryogenic Fluid In-situ Liquefaction for Landers (CryoFILL) project is an effort undertaken by NASA to develop and demonstrate a flight-representative liquefaction system using broad area cooling. A part of this effort is to develop predictive performance models that can be used to design and analyze propellant liquefaction and storage systems.

2. CryoFILL Test Hardware

The test hardware employed in the first phase of the CryoFILL project has been detailed elsewhere [2-3]. It consists of an Aluminum tank that holds a volume of 2.1 m^3. The tank is installed within the NASA GRC's Small Multipurpose Research Facility (SMiRF) thermal vacuum chamber. It is covered with insulation consisting of 40 layers of aluminized Mylar and is suspended from the vacuum chamber lid. A liquid nitrogen cooled thermal shroud, nominally at 250 K, encompasses the tank.

An integrated cryocooler system provides nearly 200 W of cooling at 90 K to a neon loop which is routed over the tank through a "tube-on-tank" heat exchanger. Manifolds at the top and bottom of the tank ensure even distribution of the flow into eight 12 mm diameter tubes. A cryofan is employed to flow neon from the top of the tank to the bottom of the tank to minimize stratification inside the tank. Gaseous oxygen is fed into the tank using a flow controller. CryoFILL instrumentations include temperature, pressure, fill level, and flow sensors. Heaters placed on the tank and the neon loop provide additional test variables.

3. CryoFILL Modeling Approach

Modeling the dynamics inside a cryogenic tank is a complex problem. There is heat transfer between the environment and the tank wall and that from the tank wall to the gas and the liquid inside the tank. Mass and heat transfer occur at the liquid-gas interface. There is heat and mass transfer between the fluid in the tank and the gas entering the tank. Lastly, heat transfer between the tank wall and the cooling flow lines must be included for modeling broad area cooling. The heat and mass transfer components involved in the liquefaction process, absent the environmental heat loads, are represented in Figure 1.

T_U – Ullage temperature
T_L – Liquid temperature
T_I – Interface temperature
A – Interface surface area
U_{UI} – Ullage to interface heat transfer coefficient
U_{LI} – Liquid to interface heat transfer coefficient
H_{vap} – Heat of vaporization

Heat Transfer Components
q_{GN2} – GN2 inflow to ullage
q_{UC} – Ullage to condensate layer
q_{CW} – Condensate layer to tank wall
q_{WN} – Tank wall to Ne flow
q_{LW} – Liquid to tank wall
q_{UI} – Ullage to interface $U_{UI}A(T_U-T_I)$
q_{LI} – Liquid to interface $U_{LI}A(T_L-T_I)$
q_{Ne} – Ne heat flow

Mass Flow Components
m_{GN2} – GN2 mass inflow
m_{CL} – Condensate layer mass flow
m_{UL} – Ullage to liquid mass flow $(q_{UI}-q_{LI})/H_{vap}$
m_{Ne} – Ne mass flow

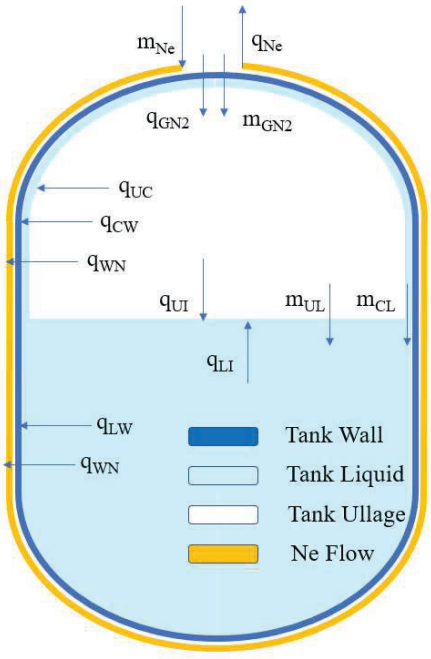

Figure 1. Schematic of liquefaction tank heat and mass transfer processes.

As the warm gas enters the tank it adds heat and mass to the ullage. Condensation occurs both on the tank wall exposed to the ullage and at the liquid/ullage interface. The heat transfer coefficient for the condensation at the tank wall is simply k/d where k is the thermal conductivity of the liquid and d is the condensate film thickness. The heat flow from the ullage to the neon is further impeded by the tank and the BAC tube walls, the thermal contact resistance between them, and the neon flow heat transfer coefficient. Similar impedances can be attributed to the

liquid portion of the tank. Heat and mass transfer at the interface are functions of the interface heat transfer coefficients, the interface surface area, and the heat of vaporization.

An analytical model of the CryoFILL test setup is developed in Thermal Desktop. Its FloCAD module allows the ability to build fluid flow models, such as piping and tanks, and model fluid heat transfer. The integrated model includes the liquefaction tank, the BAC tube network, the cryocooler/heat exchanger and the cryofan. Radiation from the environment to the wall surfaces is calculated by the RadCAD component of Thermal Desktop.

The neon flowing through the BAC tubes absorbs both internal and external heat loads on the tank wall. Thermal contact conductance between the tubes and the tank is not experimentally determined and is a model variable. During the tests the cryofan is nominally operated at 20 kRPM delivering a neon flow rate of approximately 8.4 g/s. This is obtained from dividing the cryocooler cold head cooling capacity based on its temperature by the enthalpy change across the cold head heat exchanger.

The cryocooler/heat exchanger components are not explicitly included in the model as they are not the focus of this study. Rather, they are modeled such that the neon temperature immediately downstream of the heat exchanger matches that in each test case considered.

A series of constant and transient oxygen liquefaction tests were conducted during the first phase of CryoFILL [2-3]. The CryoFILL thermal model developed was employed to compare its performance to test results [4-5]. As part of this effort, an efficiency is evaluated for all the liquefaction tests performed.

4. CryoFILL Liquefaction Efficiency

The Thermal Desktop model developed has facilitated analysis of all CryoFILL tests several of which are discussed here. An objective in the analysis of the CryoFILL liquefaction tests is to determine the liquefaction efficiency. A simple approach to estimate this parameter is presented. The heat removal rate (HRR) from the tank is:

*HRR = (Enthalpy of neon at BAC outlet manifold - Enthalpy of neon at BAC inlet manifold) * Neon flow rate*

In constant liquefaction tests where the tank pressure is constant the liquefaction power is:

*Liquefaction Power = (Enthalpy of incoming gas - Enthalpy of tank liquid) * Oxygen flow rate*

For variable liquefaction tests where the pressure varies the liquefaction power is:

*Liquefaction Power = (Enthalpy of incoming gas - Enthalpy of tank liquid) * Condensate flow rate*

Efficiency = Liquefaction Power / (HRR – Tank heater power)

Test 3 is a constant liquefaction test where the gas flow rate is the control parameter. The tank was initially 58% full and its pressure was maintained at 207 kPa (30 psia). The gaseous oxygen flow rate into the tank ullage volume was 0.27 kg/hr at the start and increased to 1.1 kg/hr after 17 hours in conjunction with reduction in tank and neon loop heater powers. Figure 2 shows the heat loads on the tank and on the neon loop to maintain a constant tank pressure. The neon flow rate was 8.3 g/s for the duration of the test.

Figures 3-5 compare model results against Test 3 data. The neon temperature in the BAC inlet and outlet manifolds is shown in Figure 3. Gaseous oxygen flow rate and tank pressure are presented in the subsequent figures.

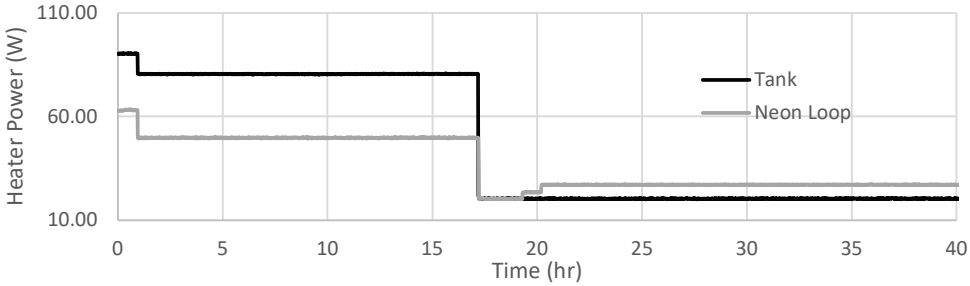

Figure 2. Test 3 – Tank and neon loop heater powers [4].

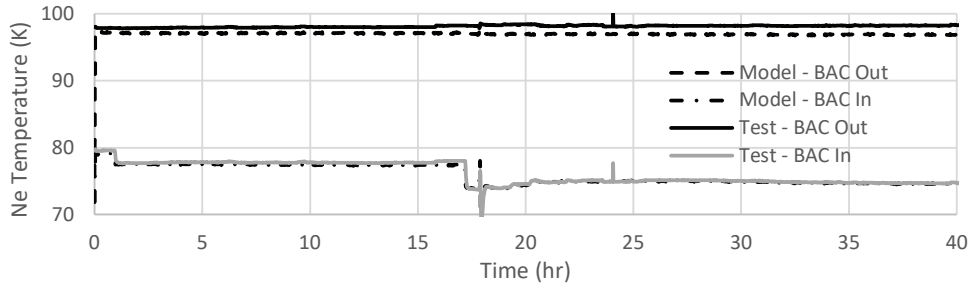

Figure 3. Test 3 – BAC neon inlet and outlet temperatures [4].

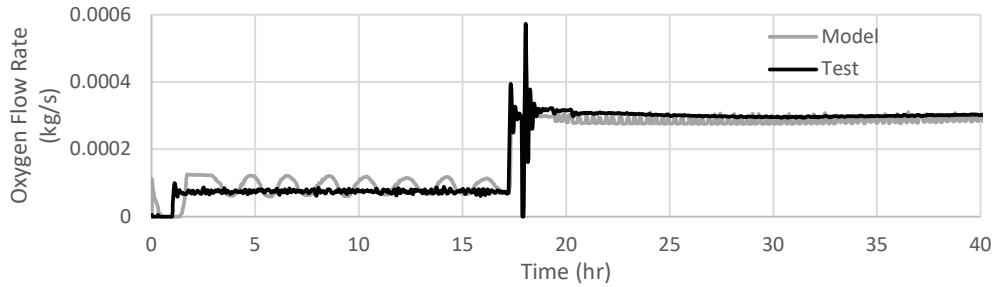

Figure 4. Test 3 – Gaseous oxygen flow rate [4].

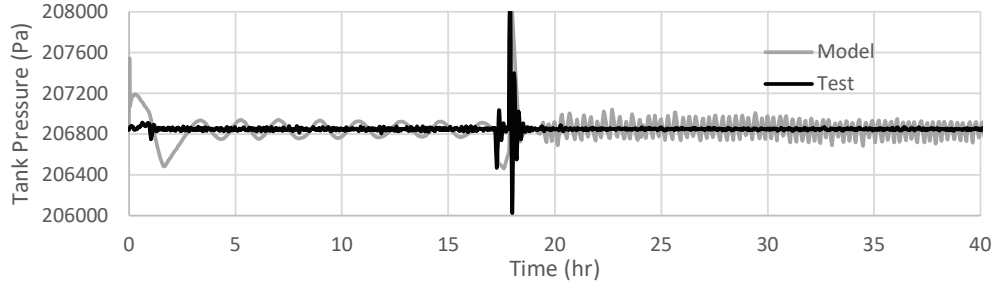

Figure 5. Test 3 – Tank pressure [4].

The model heat removal rate (HRR) is lower than that in the test due to the lower BAC outlet manifold temperature predicted by the model, Figure 6. Liquefaction power is shown in Figure 7 along with the efficiency calculated from the model results. For the constant liquefaction tests all the incoming gas is condensed thus a constant tank pressure. The efficiency calculated by the model is around 65%. This represents the efficiency of liquefaction process as it pertains to the BAC tank only.

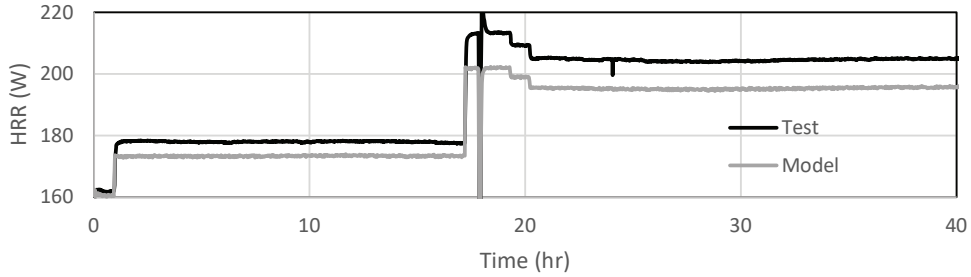

Figure 6. Test 3 – Heat removal rate.

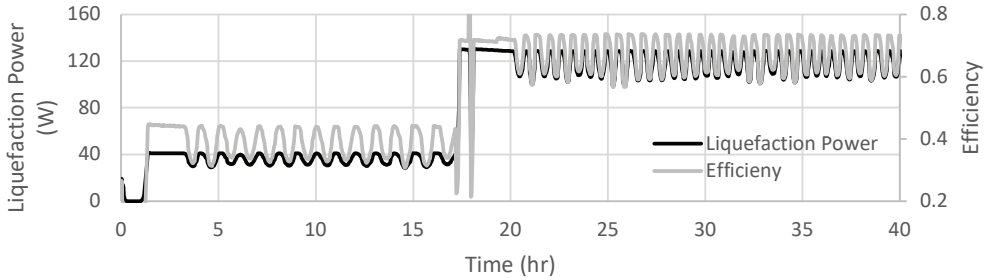

Figure 7. Test 3 – Liquefaction power and efficiency.

In the transient liquefaction part of the test matrix the effect of varying the oxygen flow rate, the environmental temperature, and the cryocooler effective heat removal rate (neon heater power) on the tank pressure was observed. Gas flow rate variation in Test 27 is provided in Figure 8. The neon flow rate was kept constant at 7.4 g/s.

The tank pressure response for this test can be seen in Figure 9. The condensate flow rate is the time rate of change of liquid mass calculated from the model results, Figure 10. The liquefaction power and efficiency are shown in Figure 11. The efficiency is higher when the oxygen flow is lower.

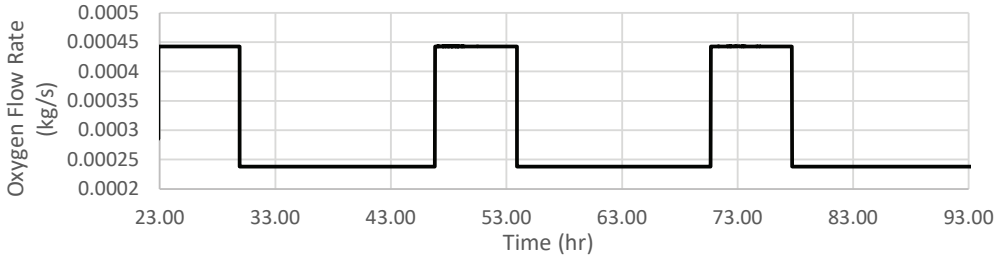

Figure 8. Test 27 – Gaseous oxygen flow rate [4].

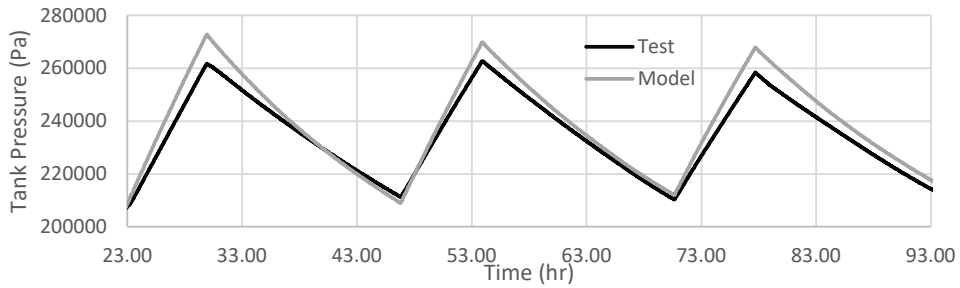

Figure 9. Test 27 – Tank pressure [4].

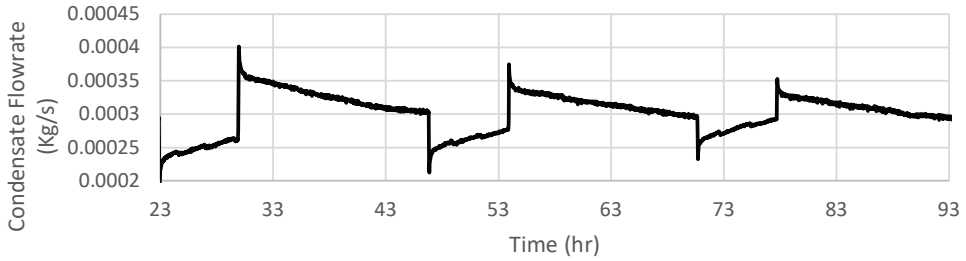

Figure 10. Test 27 – Condensate flow rate.

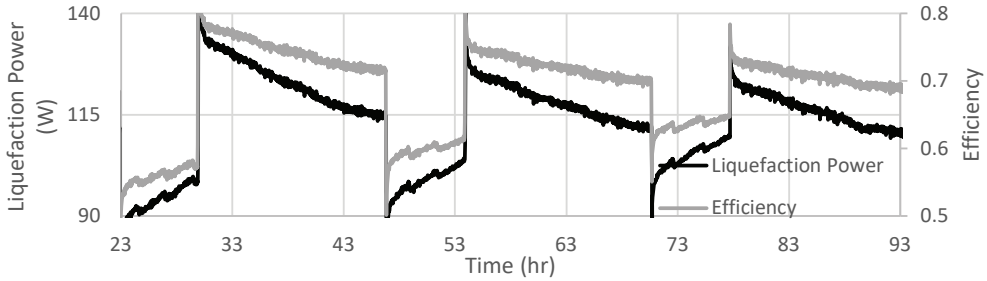

Figure 11. Test 27 – Liquefaction power and efficiency.

In Test 31 the shroud temperature varied between 225 K and 290 K, Figure 12. The tank fill level was less than 2%. The oxygen flow rate and the neon flow rate were maintained at 1.1 kg/hr and 7.2 g/s. During the pressurization periods the average pressure rate is 1.67 kPa/hr and during the depressurization periods it is -0.49 kPa/hr. The liquefaction power and efficiency for this test are shown in Figure 13. The higher efficiency correlates with the lower shroud temperature.

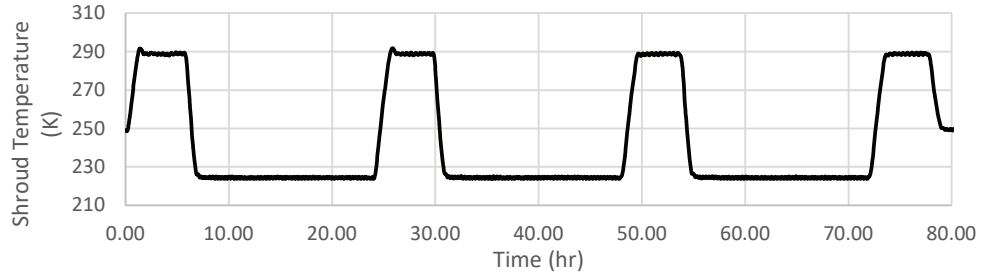

Figure 12. Test 31 – Shroud Temperature [4].

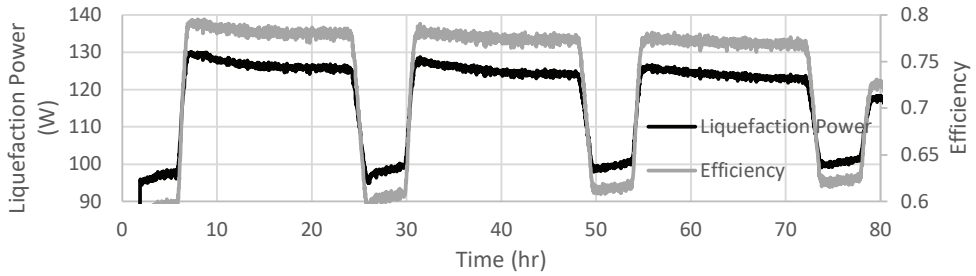

Figure 13. Test 31 – Liquefaction Power and Efficiency.

In Test 33a the tank was initially 88% full. At the start oxygen gas flow was set to 1.58 kg/hr and then lowered to 0.86 kg/hr. The tank and neon loop heaters were 20 W and 27 W, respectively. The neon flowrate was maintained at 10.5 g/s. The pressure in the test is shown in Figure 14, and the liquefaction power and efficiency are in Figure 15.

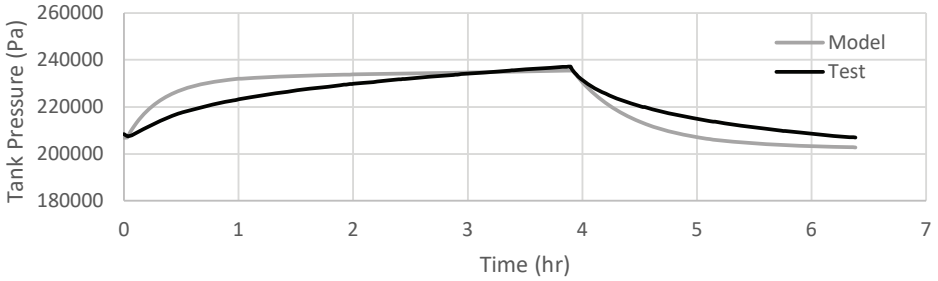

Figure 14. Test 33a – Tank pressure.

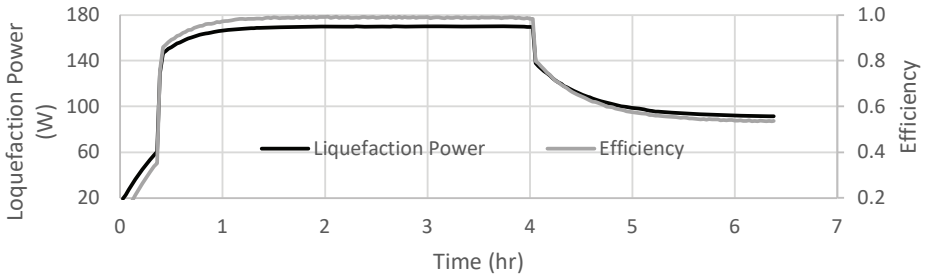

Figure 15. Test 33a – Liquefaction Power and Efficiency.

In Test 33a the liquefaction efficiency reaches near unity when the oxygen gas flow is higher. Only a small portion of the 48 W parasitic heat load imposed on the tank is removed by the neon flow. In the pressurization period the liquid temperature rises by 0.2 K which translates to an enthalpy change of 315 J/kg. Since the mass of the liquid in the tank is 2000 kg, the mean heat flow taken up by the liquid is 46 W leading to the higher than nominal liquefaction efficiency.

Test 40 was run to determine the maximum achievable liquefaction rate by turning off both the tank and neon loop heaters. In Test 40 pressure was controlled at 275 kPa (40 psia) by allowing the flowrate to vary. The gaseous oxygen flowrate was 1.6 kg/hr. The initial fill level in this test was 7% and the neon flowrate was 6.9 g/s. The liquefaction power and efficiency are shown in Figure 16.

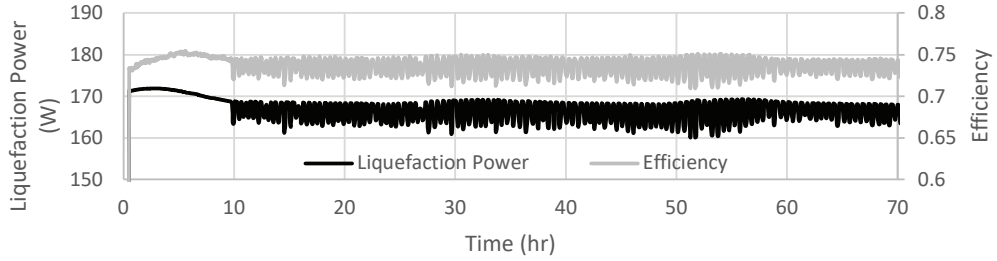

Figure 16. Test 33a – Liquefaction Power and Efficiency.

Test 5 repeated the constant liquefaction test performed in Test 3 except for the oxygen gas flow being injected by the tank dip tube into the liquid. The dip tube, approximately 5 cm above the bottom of the tank, allows the gas to bubble up through the liquid before reaching the ullage. In Test 5 the initial fill level was 65%. The neon flowrate was 8.7 g/s, and the tank and neon loop heater powers were set at 20 W and 27 W, respectively. Figure 17 compares the liquefaction efficiency for Tests 3 and 5.

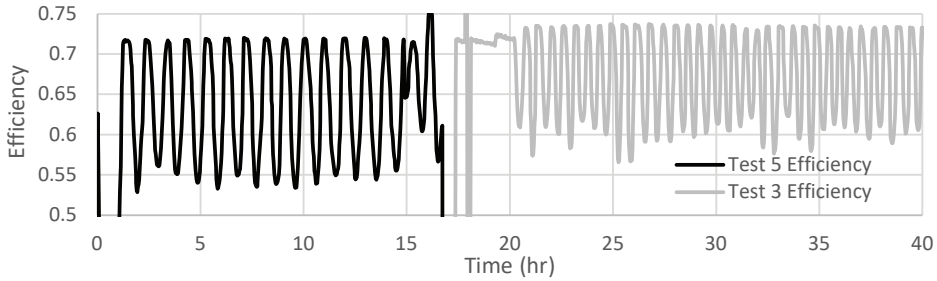

Figure 17. Comparison of Test 3 and Test 5 Liquefaction Efficiency.

5. Summary

To match the liquefaction model results to the experimental observations several model parameters had to be adjusted such as the neon flow rate, the tube to tank contact conductance, and the parasitic heat loads on the tank.

The thermal contact conductance between the BAC tubes and the tank was set to 0.1 W/cm-K. The neon flow rate calculated from the cryocooler HX temperature data was reduced by 5% to better match the model and experimental results. In modeling the liquefaction tests the total parasitic heat load on the tank had to be increased over that observed in a boil-off test that was performed prior to the liquefaction tests. The largest uncertainty in the test parameters appears to be in the parasitic heat loads.

An efficiency is calculated for all the liquefaction tests performed under the CryoFILL test series and compiled in a recent report [5]. This efficiency is a measure of the liquefaction process in the broad area cooling tank, and not an overall system efficiency that would include the cryocooler/heat exchanger system.

The efficiency in most constant liquefaction tests has a value around 0.65. In Test 40 where the tank pressure and oxygen flow are high the efficiency increases to 0.74. The efficiency of Test 5, in which the dip tube injection was employed, is slightly lower than in Test 3, its ullage injection counterpart. In transient liquefaction tests the efficiency can vary significantly during the test as the conditions in the tank change. In Tests 33a it ranges from 0.6 to near unity. The higher efficiency results from the high tank fill level.

6. References

[1] Plachta D et al 2017 Liquid Nitrogen Zero Boiloff Testing NASA/TP-2017-219389 http://ntrs.nasa.gov.
[2] Johnson W L et al 2024 IOP Conf. Ser.: Mater. Sci. Eng. **1301** 012010.
[3] Johnson W L et al 2025 Demonstration of Liquefaction for Lunar and Martian Surfaces Using Tube-on-Tank Heat Exchanger With Integrated Cryocooler and Prototype Lander Tank NASA/TP-20250000432.
[4] Kashani A et al 2024 IOP Conf. Ser.: Mater. Sci. Eng. **1301** 012009.
[5] Kashani A et al 2025 Modeling of CryoFILL Protype Liquefaction Tests NASA CFM-MODEL-RPT-051.